

Vibration analysis of boron nitride nanotubes by considering electric field and surface effect

Hamid Zeighampour¹ and Yaghoob Tadi Beni^{*2,3}

¹Mechanical Engineering Department, Shahrekord University, Shahrekord, Iran

²Faculty of Engineering, Shahrekord University, Shahrekord, Iran

³Nanotechnology Research Institute, Shahrekord University, 8818634141, Shahrekord, Iran

(Received November 27, 2020, Revised August 29, 2021, Accepted August 30, 2021)

Abstract. In this paper, the vibrations of boron nitride nanotubes (BNNTs) are investigated by considering the electric field. To consider the size effect at nanoscale dimensions, the surface elasticity theory is exploited. The equations of motion of the BNNTs are obtained by applying Hamilton's principle, and the clamped-guided boundary conditions are also considered. The governing equations and boundary conditions are discretized using the differential quadrature method (DQM), and the natural frequency is obtained by using the eigenvalue problem solution. The results are compared with the molecular dynamic simulation in order to validate the accurate values of the surface effects. In the molecular dynamics (MD) simulation, the potential between boron and nitride atoms is considered as the Tersoff type. The Timoshenko beam model is adopted to model BNNT. The vibrations of two types of zigzag and armchair BNNTs are considered. In the result section, the effects of chirality, surface elasticity modulus, surface residual tension, surface density, electric field, length, and thickness of BNNT on natural frequency are investigated. According to the results, it should be noted that, as an efficient non-classical continuum mechanic approach, the surface elasticity theory can be used in scrutinizing the dynamic behavior of BNNTs.

Keywords: boron nitride nanotubes; electric field; molecular dynamics simulation; surface elasticity theory; vibration

1. Introduction

Due to the unique mechanical, chemical, and electrical properties, boron nitride nanotubes have widespread applications in many areas (Tiano *et al.* 2014, Kim *et al.* 2018) such as polymer composite reinforcement (Zhi *et al.* 2006), aerospace applications (Thibeault *et al.* 2020), sensor, actuator (Kang *et al.* 2015), and energy applications (Nakhmanson *et al.* 2003, Sai and Mele 2003). The synthesis of BNNTs was first reported experimentally in 1994 (Rubio *et al.* 1994). The electrical properties are one of the main features of the BNNTs that distinguish them from carbon nanotube (Blase *et al.* 1994, Rubio *et al.* 1994). Comparing to the carbon nanotubes, BNNTs have better physical properties, which attract the attention of many researchers (Lee *et al.* 2001). Other nanostructures such as carbon nanotubes and graphene have different applications in the literature (Asghar *et al.* 2020, Zeverdejani and Beni 2020).

Comprehensive understanding of mechanical properties along with static and dynamic behavior of nanotubes will assist researchers to better utilize them in different applications such as nanocomposite (Faramoushjan *et al.* 2021, Heidari *et al.* 2021, Zerrouki *et al.* 2021). In nanoscale dimensions, the classical continuum mechanic is unable to accurately predict the dynamic and static behavior of nanotubes. Therefore, in recent years the researchers

have investigated the mechanical properties of nanostructures by non-classical continuum mechanics, considering the size effect. It is worth mentioning that the molecular dynamics simulation methods (Ajori and Ansari 2014) can also be used to investigate the mechanical properties of nanostructures by researchers. However, this method requires time-consuming calculations and complex analysis. Also, Experimental methods, furthermore, are too expensive, and controlling them would be too complicated in nanoscale dimensions. Therefore, molecular dynamics simulation and experimental methods would not be efficient for analyzing all nanostructures. Due to the discussed reasons, non-classical continuum mechanics would be a great candidate for researchers who are looking for a more cost-effective and accurate method. Generally, continuum mechanics has recently been used for different problems. However, at nanoscale dimensions, the classical continuum mechanics did not fit with the experimental and molecular dynamics simulation results due to the absence of size effect. Therefore, classical continuum mechanics can be modified into new theories at nanoscale dimensions by applying size effect. These theories include nonlocal theory (Hosseini-Hashemi and Ilkhani 2016, Balubaid *et al.* 2019, Berghouti *et al.* 2019, Boutaleb *et al.* 2019, Hussain *et al.* 2019, Atabakhshian and Shooshtaria 2020, Bellal *et al.* 2020, Civalek *et al.* 2020, Khosravi *et al.* 2020, Matouk *et al.* 2020, Ouakad *et al.* 2020, Rouabhia *et al.* 2020, Shariati *et al.* 2020a, Timesli 2020), strain gradient theory (Meleshko and Tokovy 2013, Tadi Beni 2016, Zeighampour *et al.* 2017, Alimirzaei *et al.* 2019, Karami *et al.* 2019a, b, Ahmed *et al.* 2020, Dehshahri *et al.* 2020), couple stress theory (Zeighampour and Beni 2014,

*Corresponding author, Professor,
E-mail: tadi@sku.ac.ir

Zeighampour *et al.* 2015, Beni 2016, Ebrahimi and Daman 2016, Ebrahimi and Beni 2016, Beni *et al.* 2017, Esmaeili and Beni 2019, Karimipour *et al.* 2019, 2020, 2021, Ghobadi *et al.* 2021a, b), and surface elasticity theory (Sahmani *et al.* 2016, Sedighi and Bozorgmehri 2016), which have attracted the attention of numerous researchers.

In this paper, the surface elasticity theory is exploited in order to investigate the vibrations of BNNTs. The surface energy creates unique properties in nanomaterials and nanostructures. As mentioned by Streitz *et al.* (1994), atoms have different behavior on a free surface or between two surfaces compared to other atoms. Moreover, the equilibrium position and energy of these atoms are different from the positions and energies of the atoms within the matter. The properties of a solid body depend on the atomic position or energy of the atoms, as a result, these properties on or between or near the surfaces are different from other parts of the matter. The effects of the surface on thin films or layered structures in which many atoms are placed near the surface or between two surfaces in two different media are significant compared to the bulk parts. Gurtin and Murdoch proposed a general theoretical framework for surface/interface energy based on the concepts of continuum mechanics. In this model, based on the mathematical model, a surface with a thickness of zero is considered and placed on the main bulk materials without slipping. Because the surface properties are different from the bulk part, these properties are specified by the surface residual tension and the surface Lamé constant (Gurtin and Murdoch 1975).

Several studies have been carried out in order to investigate the dynamic and static behavior of nanostructures by the surface elasticity theory. For example, Ansari *et al.* (2015) investigated the vibrations and stability of nanotubes conveying fluid applying surface elasticity theory. They adopted the Timoshenko beam theory to model the nanotube and indicated that the natural frequency would be greater than the classical continuum mechanics by increasing the surface elasticity theory, and this enhancement would be higher in nanotubes with fewer thicknesses. Xu *et al.* (2016) investigated the size effect on vibration and buckling of a nanobeam under electrical and magnetic loads. In this paper, size effects are considered by applying the surface elasticity theory. They evaluated the effects of stress, piezoelectric, and magnetic surfaces and represented that the stress surface effects in smaller thicknesses of nanobeam are considerable on the frequency and critical load. Pishkenari *et al.* (2015) calculated the size effects on the vibrations of a silicon nanobeam by surface elasticity theory and molecular dynamics. They demonstrated that the mechanical properties on the nanobeam surface are different relative to its center, and the results achieved from the surface elasticity theory is fitted with the molecular dynamics. Zhen (2017) investigated wave propagation in a nanotube conveying fluid using surface elasticity theory. In his study, the nonlocal effects are considered by applying the nonlocal theory. He indicated that the effects of surface elasticity theory and surface residual tension on the wave propagation of nanobeam are significant in smaller wavenumbers and

diameters. Attia (2017) investigated bending, buckling, and vibration of scaled nanobeam by surface elasticity theory. He suggested that the effects of surface energy would be higher with increasing the ratio of length to thickness. Moreover, the effect of surface energy is greater on bending and buckling than the vibrations.

Molecular dynamics have widespread applications in atomic simulation. In this method, the equations of the interaction of molecules and atoms in a certain time period are achieved from Newton's second law, and the aim is to solve these equations. In this technique, atomic simulation is performed by the actual form of nanostructures, thus, the results obtained from this method have good accuracy. Considering that materials and structures in a variety of engineering applications are usually divided into multi-micron scales and contain billions of atoms, atomic simulation and analysis of such structures are complicated due to computational constraints. The molecular dynamics method has been recently exploited to simulate the mechanical properties and dynamic behavior of piezoelectric nanostructures. For example, Zhang *et al.* (2013a) investigated the buckling and failure of a Silicon carbide nanobeam in a different electric field by molecular dynamics. They revealed that the electric field would have a considerable impact on the critical load and failure strain. Moreover, they compared the simulation results with the nonlocal theory and demonstrated that classical continuum mechanics approach is not accurate to evaluate the behavior of nanostructures. Zhang and Wang (2014) investigated the effects of the electric field on the mechanical properties of gallium nitride by molecular dynamics simulation. They represented that the negative electric field leads to a reduction in the failure strength and strain, and Young's modulus declines by reducing the electric field. Zhang *et al.* (2013b) investigated the pre-buckling and buckling of BNNTs and boron nitride nanosheets by applying molecular mechanics. In their study, the effects of the electric field are intended. They indicated that the electric field generates an axial deformation in zigzag nanostructures and a shear deformation in armchair nanostructures. This is because of the different polarization behavior of each of the nanostructures in the case that there is an electric field. Chandra *et al.* (2016) investigated the effect of temperature on the buckling of BNNTs by applying molecular dynamics method. They indicated that the type of nanotube chirality influences its critical temperature, and the resistance of zigzag BNNTs against buckling is more than that of the armchair. Chandra *et al.* (2015) examined the effects of temperature on vibrations of BNNTs by using molecular dynamics simulation and demonstrated that the natural frequency of the BNNT decreases by increasing the temperature, and also the effect of temperature on the frequency of the BNNT in smaller lengths is considerable.

In this paper, the DQM method is employed to solve the problem. In recent years, this method has gained much attention from researchers (Al-Furjan *et al.* 2020a, b, c, d, Shariati *et al.* 2020b). For example, using the couple stress theory and the Donnell shell model, Zeighampour and Tadi Beni (2014) studied the vibrations of nanotubes conveying a fluid. Applying the DQM method, they also solved the

vibration problem. In another work, using strain gradient theory, Zeighampour and Beni (2015) examined the vibration of axially functionally graded nanobeam. They also used the DQM method to solve the problem. Using couple stress theory, Shojaeian and Beni (2015) examined electromechanical buckling of functionally graded electrostatic nano-bridges in their study. They also discretized and investigated nonlinear equations employing the DQM method. De Rosa *et al.* (2021) studied the vibrations of nonuniform carbon nanotube with elastic constraints and an attached mass based on nonlocal theory. Using the DQM, they discretized the equations and calculated the natural frequency. Huang *et al.* (2021) examined rotary functionally graded microsystem. In their work, they used the DQM method to solve the vibration problem. Al-Furjan *et al.* (2021b) employed refined high-order theory to investigate the bending responses of a functionally graded-graphene nanoplatelets composite reinforced disk. They also solved their problem by the DQM. Al-Furjan *et al.* (2021a) examined the vibrations of the imperfect sandwich higher-order disk with a lactic core using the DQM method. They evaluated various parameters such as boundary conditions, outer to inner radius ratio, honeycomb network angle, thickness to length ratio of the honeycomb, fibers angle, weight fraction of carbon nanotubes of disk in their work.

According to the foregoing discussion, the effect of electric field on vibrations of BNNTs by using surface elasticity theory and molecular dynamics has rarely been considered by researchers, therefore, this problem is addressed in this paper. Moreover, to verify the accuracy of surface elasticity theory and compare the results, the molecular dynamics method is exploited in this paper. The Timoshenko beam model is adopted to model BNNT. The two types of zigzag and armchair BNNTs are considered in order to evaluate the effect of the electric field on natural frequency. Furthermore, it is shown that the electric field effects are different depending on the arrangement of the atoms in BNNT.

2. Modeling of boron nitride nanotube

2.1 Modeling based on molecular dynamics simulation

BNNTs are formed by twisting of boron nitride sheet (Rubio *et al.* 1994). Zigzag and armchair BNNTs are displayed as $(n, 0)$, and (n, n) , respectively. The visual molecular dynamics software is used to model BNNTs. In this paper, the large-scale atomic/molecular massively parallel simulator (LAMMPS) software is used for molecular dynamics simulation. Before utilizing molecular dynamics simulation, the conjugate gradient algorithm is employed to minimize the energy from the residual tensions in BNNTs. The integration of the equations of motion is carried out by using the velocity Verlet algorithm with an interval of 1 fs. The Nose-Hoover thermostat is used to control the temperature. To simulate the boundary conditions, two rows of atoms are fixed. After the free vibration of the

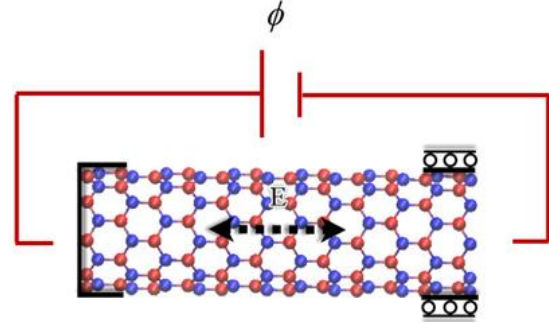


Fig. 1 Boundary conditions and electric field of the BNNT

BNNT, the displacement of the center of mass of the BNNT relative to the time is extracted. Then, the natural frequency of BNNTs is computed by using the fast Fourier transform method.

In Tersoff potential, electrostatic interactions are not considered (López-Suárez *et al.* 2015). To simulate an electric field, the force from this field should be applied to the BNNT, which is equivalent to $f_i = E \times q_i$ where q_i is the charge of each atom. It should be noted that the charge values of B and N are 2.7 and -2.7, respectively. These values are obtained by using density functional theory (DFT) calculations for hexagonal boron nitride (h-BN) (Ohba *et al.* 2001) and BNNTs (Nakhmanson *et al.* 2003). Electric field and the boundary conditions of BNNT is represented in Fig. 1.

2.2 Modeling based on surface elasticity theory

In this section, the governing equations for the vibrations of BNNTs are extracted based on the Timoshenko beam model, and the equations of motion and boundary conditions are extracted for BNNTs. The strain energy of the BNNTs is defined as follows based on the surface elasticity theory in the enclosed volume V (Zhu *et al.* 2017).

$$U_{s,e} = \frac{1}{2} \int_V (\sigma_{ij} \varepsilon_{ij} - D_i E_i) dV + \frac{1}{2} \left(\int_{S^+} (\sigma_{ij}^s \varepsilon_{ij} - D_i^s E_i) dS^+ + \int_{S^-} (\sigma_{ij}^s \varepsilon_{ij} - D_i^s E_i) dS^- \right) \quad (1)$$

In the above equation, σ_{ij} , σ_{ij}^s , ε_{ij} , D_i , D_i^s and E_i are the components of Cauchy stress tensor, surface stress tensor, strain tensor, electric displacement, surface electric displacement and electric field vector, respectively, which are expressed as follows:

$$\begin{aligned} \sigma_{ij} &= C_{ijkl} \varepsilon_{kl} - e_{ijm} E_m \\ D_m &= e_{ijm} \varepsilon_{ij} + \eta_{mk} E_k \end{aligned} \quad (2)$$

$$\varepsilon_{ij} = \frac{1}{2} (u_{i,j} + u_{j,i}), \quad (3)$$

where C_{ijkl} , e_{ijm} , η_{mk} and u_i represent, the components of elastic constants, piezoelectric constants, dielectric constants and the displacement vector components, respectively.

The stress-strain relations based on the surface elasticity theory are expressed as follows:

$$\begin{aligned}\sigma_{ij}^s &= \tau^s \delta_{ij} + (\tau^s + \lambda^s) \varepsilon_{kk} \delta_{ij} \\ &+ 2(\mu^s - \tau^s) \varepsilon_{ij} + \tau^s u_{z,i}^s - e_{ijm}^s E_m, \\ \sigma_{iz}^s &= \tau^s u_{z,i}^s; \quad (i, j = x, y) \\ D_m^s &= e_{ijm}^s \varepsilon_{ij} + \eta_{mk}^s E_k,\end{aligned}\quad (4)$$

where τ^s , μ^s , λ^s , e_{ijm}^s and η_{mk}^s represent, the surface residual tension, surface Lamé's constants, surface piezoelectric constants and surface dielectric constants.

In the recent years, different beam theories have attracted considerable attention in the investigation of the dynamic behavior of nano/microstructure. These theories include Euler–Bernoulli (Heireche *et al.* 2008), Timoshenko (Draiche *et al.* 2019) and integral-first shear deformation (Bourada *et al.* 2020, Bousahla *et al.* 2020, Rouabhia *et al.* 2020) beam theories. In this paper, The Timoshenko beam theory is used to model BNNT. Besides, \mathbf{u} is the displacement vector based on Timoshenko beam is as follows:

$$\mathbf{u} = \begin{cases} u_1 = u(x) + z\psi(x) \\ u_2 = 0 \\ u_3 = w(x) \end{cases} \quad (5)$$

In which, u_1 , u_2 and u_3 denote the displacement along the axes x , y , and z , respectively, for a desired element of the beam. Also, w is the transverse displacement, ψ is the rotation of the cross section of the beam around the y axis. By substituting the Eq. (5) in Eqs. (2) and (3), the strain and stress along with the electric field and the electric displacement are obtained as follows:

$$\varepsilon_{xx} = \frac{\partial u}{\partial x} + \frac{1}{2} \left(\frac{\partial w}{\partial x} \right)^2 + z \frac{\partial \psi}{\partial x}, \quad (6)$$

$$\varepsilon_{xz} = \frac{1}{2} \left(\psi + \frac{\partial w}{\partial x} \right), \quad (7)$$

$$\sigma_{xx} = (\lambda + 2\mu) \varepsilon_{xx} - e_{xxx} E_x, \quad (8)$$

$$\begin{aligned}\sigma_{xz} &= \mu \left(\psi + \frac{\partial w}{\partial x} \right) - e_{xzx} E_x, \\ D_x &= e_{xxx} \varepsilon_{xx} + 2e_{xzx} \varepsilon_{xz} + \eta_{xx} E_x\end{aligned}\quad (9)$$

$$E_x = -\frac{\partial \phi}{\partial x} \quad (10)$$

where, ϕ represent the electric potential.

Also, the stress and the surface electric displacement according to Eq. (4) are obtained as follows:

$$\begin{aligned}\sigma_{xx}^s &= \tau^s - \frac{\tau^s}{2} \left(\frac{\partial w}{\partial x} \right)^2 + (\lambda_s + 2\mu_s) \varepsilon_{xx} - e_{xxx}^s E_x, \\ \sigma_{xz}^s &= \tau^s \frac{\partial w}{\partial x}\end{aligned}\quad (11)$$

$$D_x^s = e_{xxx}^s \varepsilon_{xx} + 2e_{xzx}^s \varepsilon_{xz} + \eta_{xx}^s E_x \quad (12)$$

$$E_x = -\frac{\partial \phi}{\partial x} \quad (13)$$

In the classical beam theory, the stress σ_{zz} versus the stresses σ_{xx} , σ_{xz} is small and negligible. However, in the surface elasticity theory, this assumption is not true. Therefore, it is assumed that the stress σ_{zz} linearly changes in the direction of the thickness. According to this assumption, stress σ_{zz} is obtained as follows (Ansari *et al.* 2014):

$$\begin{aligned}\sigma_{zz} &= \left(\frac{h+2}{2h} \right) \left(\frac{\partial \sigma_{xz}^{S^+}}{\partial x} - \rho_{s^+} \frac{\partial^2 w}{\partial t^2} \right) \\ &- \left(\frac{h-2z}{2h} \right) \left(\frac{\partial \sigma_{xz}^{S^-}}{\partial x} - \rho_{s^-} \frac{\partial^2 w}{\partial t^2} \right)\end{aligned}\quad (14)$$

where the superscripts S^+ and S^- represent to the outer and inner surfaces of BNNT, respectively. Also, h is the BNNT thickness.

By substituting Eq. (11) in Eq. (14), σ_{zz} can be expressed as follows:

$$\sigma_{zz} = \frac{2z}{h} \left(\tau^s \frac{\partial^2 w}{\partial x^2} - \rho_s \frac{\partial^2 w}{\partial t^2} \right) \quad (15)$$

Eq. (8) for a bulk BNNT can be described as follows:

$$\begin{aligned}\sigma_{xx} &= (\lambda + 2\mu) \varepsilon_{xx} + \frac{2\nu z}{(1-\nu)h} \left(\tau^s \frac{\partial^2 w}{\partial x^2} - \rho_s \frac{\partial^2 w}{\partial t^2} \right) \\ &- e_{xxx} E_x,\end{aligned}\quad (16)$$

In which by substituting Eq. (15) in Eq. (16), the stress can be stated as follows:

$$\sigma_{xx} = (\lambda + 2\mu) \varepsilon_{xx} + \frac{2\nu z \tau^s}{(1-\nu)h} \frac{\partial^2 w}{\partial x^2} - e_{xxx} E_x, \quad (17)$$

To derive the equations of motion of the BNNT, strain energy and work of external forces are needed that the work due to axial force N_0 is defined as follows:

$$W = (N_0 u) \Big|_{x=0}^{x=L} \quad (18)$$

The kinetic energy of BNNT is as follows.

$$\begin{aligned}T &= \frac{1}{2} \int_0^L \left\{ [\rho A + \pi(d_i + d_o)\rho_s] \left[\left(\frac{\partial u}{\partial t} \right)^2 + \left(\frac{\partial w}{\partial t} \right)^2 \right] \right. \\ &\quad \left. + \left[\rho I + \frac{\pi \rho_s (d_i^3 + d_o^3)}{8} \right] \left(\frac{\partial \psi}{\partial t} \right)^2 \right\} dx\end{aligned}\quad (19)$$

In which ρ_s, ρ are surface density and BNNT density, respectively. A, I are the cross-section and the moment of inertia of BNNT, respectively.

Now, using the principle of minimum potential energy $\delta(U_{s,e} - W - T) = 0$, the equations of motion and boundary conditions are obtained as follows:

$$\begin{aligned}\delta u: \quad &\frac{\partial(N_{xx} + \bar{N}_{xx})}{\partial x} = [\rho A + \pi \rho_s (d_i + d_o)] \frac{\partial^2 u}{\partial t^2}, \\ \delta w: \quad &\frac{\partial}{\partial x} \left((N_{xx} + \bar{N}_{xx}) \frac{\partial w}{\partial x} \right) + \frac{\partial(Q_{xz} + \bar{Q}_{xz})}{\partial x} \\ &= [\rho A + \pi \rho_s (d_i + d_o)] \frac{\partial^2 w}{\partial t^2},\end{aligned}\quad (20)$$

$$\begin{aligned} \delta\psi: & \frac{\partial(M_{xx} + \bar{M}_{xx})}{\partial x} - Q_{xz} \\ = & \left[\rho I + \frac{\pi\rho_s(d_i^3 + d_o^3)}{8} \right] \frac{\partial^2\psi}{\partial t^2} + \left[\frac{2\nu I\rho_s}{(1-\nu)h} \right] \frac{\partial^3 w}{\partial x \partial t^2}, \\ \delta\phi: & \frac{\partial(D_x + \bar{D}_x)}{\partial x} = 0 \end{aligned}$$

$$\begin{aligned} N_{xx} + \bar{N}_{xx} - N_0 = 0 \quad \text{or} \quad u = 0, \quad x = 0, L \\ (N_{xx} + \bar{N}_{xx}) \frac{\partial w}{\partial x} + Q_{xz} + \bar{Q}_{xz} = 0 \\ \text{or} \quad w = 0, \quad x = 0, L \end{aligned} \quad (21)$$

$$\begin{aligned} M_{xx} + \bar{M}_{xx} = 0 \quad \text{or} \quad \psi = 0, \quad x = 0, L \\ D_x + \bar{D}_x = 0 \quad \text{or} \quad \phi = 0, \quad x = 0, L \end{aligned} \quad (22)$$

where

$$\begin{aligned} N_{xx} &= a_1 \left(\frac{\partial u}{\partial x} + \frac{1}{2} \left(\frac{\partial w}{\partial x} \right)^2 \right) + a_2 \frac{\partial \phi}{\partial x}, M_{xx} \\ &= a_3 \frac{\partial \psi}{\partial x} + a_4 \frac{\partial^2 w}{\partial x^2}, Q_{xz} = a_5 \left(\psi + \frac{\partial w}{\partial x} \right) + a_6 \frac{\partial \phi}{\partial x} \\ D_x &= e_{xxx} \left(\frac{\partial u}{\partial x} + \frac{1}{2} \left(\frac{\partial w}{\partial x} \right)^2 \right) + e_{xzx} \left(\psi + \frac{\partial w}{\partial x} \right) - \eta_{xx} \frac{\partial \phi}{\partial x} \end{aligned} \quad (23)$$

$$\begin{aligned} a_1 &= (\lambda + 2\mu)A, a_2 = e_{xxx}A, a_3 = (\lambda + 2\mu)I, \\ a_4 &= \frac{2\nu I \tau^s}{(1-\nu)h}, a_5 = k_s \mu A, a_6 = e_{xzx}A \end{aligned}$$

$$\begin{aligned} \bar{N}_{xx} &= a_{s1} \left(\frac{\partial u}{\partial x} + \frac{1}{2} \left(\frac{\partial w}{\partial x} \right)^2 \right) + a_{s2} \frac{\partial \phi}{\partial x} + a_{s3} \left(\frac{\partial w}{\partial x} \right)^2 \\ + a_{s4}, \bar{M}_{xx} &= a_{s5} \frac{\partial \psi}{\partial x}, \bar{Q}_{xz} = a_{s4} \frac{\partial w}{\partial x} \\ \bar{D}_x &= e_{xxx}^s \left(\frac{\partial u}{\partial x} + \frac{1}{2} \left(\frac{\partial w}{\partial x} \right)^2 \right) + e_{xzx}^s \left(\psi + \frac{\partial w}{\partial x} \right) - \eta_{xx}^s \frac{\partial \phi}{\partial x} \end{aligned} \quad (24)$$

$$\begin{aligned} a_{s1} &= \pi(d_i + d_o)(\lambda_s + 2\mu_s), \\ a_{s2} &= e_{xxx}^s \pi(d_i + d_o), a_{s3} = -\frac{\tau_s \pi(d_i + d_o)}{2} \\ a_{s4} &= \tau_s \pi(d_i + d_o), a_{s5} = \frac{\pi(d_i^3 + d_o^3)}{8} (\lambda_s + 2\mu_s) \end{aligned}$$

By substituting Eqs. (23) and (24) in Eqs. (20)-(22), the equations of motion based on the displacement components can be rewritten as follows:

$$\begin{aligned} \delta u: & \frac{\partial}{\partial x} \left(\begin{aligned} & (a_1 + a_{s1}) \left(\frac{\partial u}{\partial x} + \frac{1}{2} \left(\frac{\partial w}{\partial x} \right)^2 \right) \\ & + (a_2 + a_{s2}) \frac{\partial \phi}{\partial x} + a_{s3} \left(\frac{\partial w}{\partial x} \right)^2 + a_{s4} \end{aligned} \right) \\ & = [\rho A + \pi(d_i + d_o)\rho_s] \frac{\partial^2 u}{\partial t^2}, \\ \delta w: & \left((a_1 + a_{s1}) \frac{\partial^2 u}{\partial x^2} + (a_2 + a_{s2}) \frac{\partial^2 \phi}{\partial x^2} \right. \\ & \left. + (a_1 + a_{s1} + 2a_{s3}) \frac{\partial w}{\partial x} \frac{\partial^2 w}{\partial x^2} \right) \frac{\partial w}{\partial x} \\ & + \left(\begin{aligned} & (a_1 + a_{s1}) \left(\frac{\partial u}{\partial x} + \frac{1}{2} \left(\frac{\partial w}{\partial x} \right)^2 \right) \\ & + (a_2 + a_{s2}) \frac{\partial \phi}{\partial x} + a_{s3} \left(\frac{\partial w}{\partial x} \right)^2 + a_{s4} \end{aligned} \right) \frac{\partial^2 w}{\partial x^2} \end{aligned} \quad (25)$$

$$\begin{aligned} + a_5 \left(\frac{\partial \psi}{\partial x} + \frac{\partial^2 w}{\partial x^2} \right) + a_6 \frac{\partial^2 \phi}{\partial x^2} + a_{s4} \frac{\partial^2 w}{\partial x^2} \\ = [\rho A + \pi(d_i + d_o)\rho_s] \frac{\partial^2 w}{\partial t^2}, \end{aligned}$$

$$\begin{aligned} \delta\psi: & (a_3 + a_{s5}) \frac{\partial^2 \psi}{\partial x^2} + a_4 \frac{\partial^3 w}{\partial x^3} - a_5 \left(\psi + \frac{\partial w}{\partial x} \right) - a_6 \frac{\partial \phi}{\partial x} \\ = & \left[\rho I + \frac{\pi\rho_s(d_i^3 + d_o^3)}{8} \right] \frac{\partial^2 \psi}{\partial t^2} + \left[\frac{2\nu I\rho_s}{(1-\nu)h} \right] \frac{\partial^3 w}{\partial x \partial t^2}, \\ \delta\phi: & (e_{xxx} + e_{xxx}^s) \left(\frac{\partial^2 u}{\partial x^2} + \frac{\partial^2 w}{\partial x^2} \frac{\partial w}{\partial x} \right) \\ & + (e_{xzx} + e_{xzx}^s) \left(\frac{\partial \psi}{\partial x} + \frac{\partial^2 w}{\partial x^2} \right) - (\eta_{xx} + \eta_{xx}^s) \frac{\partial^2 \phi}{\partial x^2} = 0 \end{aligned}$$

The boundary conditions for zigzag and armchair BNNTs are as follows:

$$\begin{aligned} w = 0, \quad x = 0, L \\ \psi = 0, \quad x = 0, L \\ D_x = 0, \quad x = 0, L \end{aligned} \quad (26)$$

To analyze the vibrations of BNNTs, considering that the acceleration in longitudinal direction is negligible with respect to transvers direction. By using Eq. (25), the longitudinal displacement of the BNNT can be expressed as follows:

$$\begin{aligned} u(x) &= -\frac{(a_2 + a_{s2})}{(a_1 + a_{s1})} \phi(x) - \left(\frac{1}{2} + \frac{a_{s3}}{(a_1 + a_{s1})} \right) \\ & \int_0^x \left(\frac{\partial w}{\partial x} \right)^2 dx + \left(\frac{a_{s4}}{(a_1 + a_{s1})} + C_1 \right) x + C_2 \end{aligned} \quad (27)$$

In the above equation, C_1 and C_2 are constant values that are extracted from the boundary conditions. By substituting boundary conditions in Eq. (27), C_1 and C_2 are extracted as follows:

$$\begin{aligned} x = 0, \quad U = 0, \quad C_2 = \frac{(a_2 + a_{s2})}{(a_1 + a_{s1})} \phi(0) \\ x = L, \quad N_0 = -N_E, \quad C_1 = -N_E \end{aligned} \quad (28)$$

The equations of motion of the BNNT can be rewritten using Eqs. (27) and (28) as follows:

$$\begin{aligned} \delta w: & (-N_E) \frac{\partial^2 w}{\partial x^2} + a_5 \left(\frac{\partial \psi}{\partial x} + \frac{\partial^2 w}{\partial x^2} \right) + a_6 \frac{\partial^2 \phi}{\partial x^2} \\ & + a_{s4} \frac{\partial^2 w}{\partial x^2} = [\rho A + \pi(d_i + d_o)\rho_s] \frac{\partial^2 w}{\partial t^2}, \\ \delta\psi: & (a_3 + a_{s5}) \frac{\partial^2 \psi}{\partial x^2} + a_4 \frac{\partial^3 w}{\partial x^3} - a_5 \left(\psi + \frac{\partial w}{\partial x} \right) - a_6 \frac{\partial \phi}{\partial x} \\ = & \left[\rho I + \frac{\pi\rho_s(d_i^3 + d_o^3)}{8} \right] \frac{\partial^2 \psi}{\partial t^2} + \left[\frac{2\nu I\rho_s}{(1-\nu)h} \right] \frac{\partial^3 w}{\partial x \partial t^2}, \\ \delta\phi: & (e_{xxx} + e_{xxx}^s) \left(\frac{\partial^2 u}{\partial x^2} + \frac{\partial^2 w}{\partial x^2} \frac{\partial w}{\partial x} \right) \\ & + (e_{xzx} + e_{xzx}^s) \left(\frac{\partial \psi}{\partial x} + \frac{\partial^2 w}{\partial x^2} \right) - (\eta_{xx} + \eta_{xx}^s) \frac{\partial^2 \phi}{\partial x^2} = 0 \end{aligned} \quad (29)$$

According to the arrangement of the atoms in BNNTs, the electric field in the zigzag BNNT generates a longitudinal piezoelectric response for uniaxial strain while it creates an electric dipole moment linearly coupled to torsion in the armchair BNNT. Therefore, the piezoelectric

coefficients in zigzag BNNTs are $e_{xxx} \neq 0, e_{xzx} = 0$, and the coefficients in armchair BNNTs are $e_{xxx} = 0, e_{xzx} \neq 0$, (Ohba *et al.* 2001). Hence, the equations of motion and boundary conditions, concerning the values of the mechanical properties listed, can be again rewritten as follows, respectively:

The equations of motion for zigzag BNNT:

$$\delta w: (-N_E) \frac{\partial^2 w}{\partial x^2} + a_5 \left(\frac{\partial \psi}{\partial x} + \frac{\partial^2 w}{\partial x^2} \right) + a_6 \frac{\partial^2 \phi}{\partial x^2} + a_{s4} \frac{\partial^2 w}{\partial x^2} = [\rho A + \pi(d_i + d_o)\rho_s] \frac{\partial^2 w}{\partial t^2},$$

$$\delta \psi: (a_3 + a_{s5}) \frac{\partial^2 \psi}{\partial x^2} + a_4 \frac{\partial^3 w}{\partial x^3} - a_5 \left(\psi + \frac{\partial w}{\partial x} \right) = \left[\rho I + \frac{\pi \rho_s (d_i^3 + d_o^3)}{8} \right] \frac{\partial^2 \psi}{\partial t^2} + \left[\frac{2\nu I \rho_s}{(1-\nu)h} \right] \frac{\partial^3 w}{\partial x \partial t^2}, \quad (30)$$

$$\delta \phi: \left((e_{xxx} + e_{xxx}^s) \frac{a_2 + a_{s2}}{a_1 + a_{s1}} + (\eta_{xx} + \eta_{xx}^s) \right) \frac{\partial^2 \phi}{\partial x^2} + \left((e_{xzx} + e_{xzx}^s) \frac{2a_{s3}}{a_1 + a_{s1}} \right) \frac{\partial w}{\partial x} \frac{\partial^2 w}{\partial x^2} = 0$$

The equations of motion for armchair BNNT:

$$\delta w: (a_5 + a_{s4}) \frac{\partial^2 w}{\partial x^2} + a_5 \frac{\partial \psi}{\partial x} + a_6 \frac{\partial^2 \phi}{\partial x^2} = [\rho A + \pi(d_i + d_o)\rho_s] \frac{\partial^2 w}{\partial t^2},$$

$$\delta \psi: (a_3 + a_{s5}) \frac{\partial^2 \psi}{\partial x^2} + a_4 \frac{\partial^3 w}{\partial x^3} - a_5 \left(\psi + \frac{\partial w}{\partial x} \right) - a_6 \frac{\partial \phi}{\partial x} = \left[\rho I + \frac{\pi \rho_s (d_i^3 + d_o^3)}{8} \right] \frac{\partial^2 \psi}{\partial t^2} + \left[\frac{2\nu I \rho_s}{(1-\nu)h} \right] \frac{\partial^3 w}{\partial x \partial t^2}, \quad (31)$$

$$\delta \phi: (e_{xzx} + e_{xzx}^s) \left(\frac{\partial \psi}{\partial x} + \frac{\partial^2 w}{\partial x^2} \right) - (\eta_{xx} + \eta_{xx}^s) \frac{\partial^2 \phi}{\partial x^2} = 0$$

3. Problem-solving method

The differential quadrature method is exploited to solve the equations. In this method, the expression of the derivative of a function relative at a given point as a weighted linear summation of the values of the function at all the points in the domain. The K-th derivative of the W_i, Ψ_i, Φ_i functions is approximated as follows (Shu 2000, Zong and Zhang 2009).

$$\frac{\partial^k}{\partial \zeta^k} \{W_i, \Psi_i, \Phi_i\} |_{\zeta=\zeta_j} = \sum_{m=1}^N C_{jm}^{(k)} \{W_i(\zeta_{im}, t), \Psi_i(\zeta_{im}, t), \Phi_i(\zeta_{im}, t)\} \quad (32)$$

In which N is the nodes in the domain, and $C_{jm}^{(k)}$ is the weighted coefficients obtained from recursive equations. The m -th point coordinates are achieved from the Chebyshev-Gauss-Lobatto equation (Zong and Zhang 2009).

$$\zeta_m = \frac{1}{2} \left[1 - \cos \left(\frac{m-1}{N-1} \pi \right) \right], \quad m = 1, 2, \dots, N \quad (33)$$

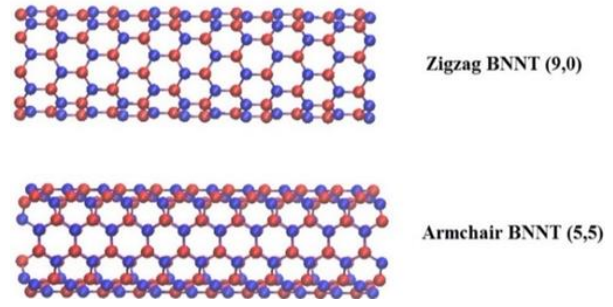


Fig. 2 (9,0) zigzag and (5,5) armchair BNNTs

Table 1 The diameter and the number of atoms of the BNNTs

	(5,5)	(9,0)
Number of atom	400	432
Diameter (nm)	0.6781	0.7047

By substituting Eq. (32) in Eqs. (26), (30) and (31) in matrix form, it is as follows:

$$\begin{bmatrix} K_{dd} & K_{db} \\ K_{bd} & K_{bb} \end{bmatrix} \begin{Bmatrix} d_d \\ d_b \end{Bmatrix} + \begin{bmatrix} M_{dd} & M_{db} \\ 0 & 0 \end{bmatrix} \begin{Bmatrix} \ddot{d}_d \\ \ddot{d}_b \end{Bmatrix} = 0 \quad (34)$$

In the above equation, the subscript d is related to the domain, and the subscript b is related to the boundary conditions. The following equation is employed to solve the equations.

$$\{d_d, d_b\} = \{\tilde{d}_d, \tilde{d}_b\} e^{\omega t} \quad (35)$$

By substituting Eq. (35) in Eq. (34), we will have:

$$(\mathbf{K} + \omega^2 \mathbf{M}) \begin{Bmatrix} \tilde{d}_d \\ \tilde{d}_b \end{Bmatrix} = 0 \quad (36)$$

In which \mathbf{K} and \mathbf{M} are the stiffness and the mass matrix, respectively. The natural frequency is obtained by using the eigenvalue problem solution of Eq. (36).

4. Results

In this section, the results of the vibrations of BNNT under an electric field are represented for different values of length, chirality, and diameter. In Fig. 2, two samples of armchair BNNTs (5,5) and zigzag BNNTs (9,0) are represented. Moreover, the geometrical and structural specifications of the BNNT used in this paper are expressed based on Table 1.

4.1 Comparison of results

In this section, the results related to natural frequency are calculated by using two methods of continuum mechanics and molecular dynamics. As previously stated, DQM is used to solve the equations. First, the number of nodes required for the convergence of the problem solution is calculated according to Fig. 3 for two BNNTs, and the natural frequency of the two BNNTs is calculated based on

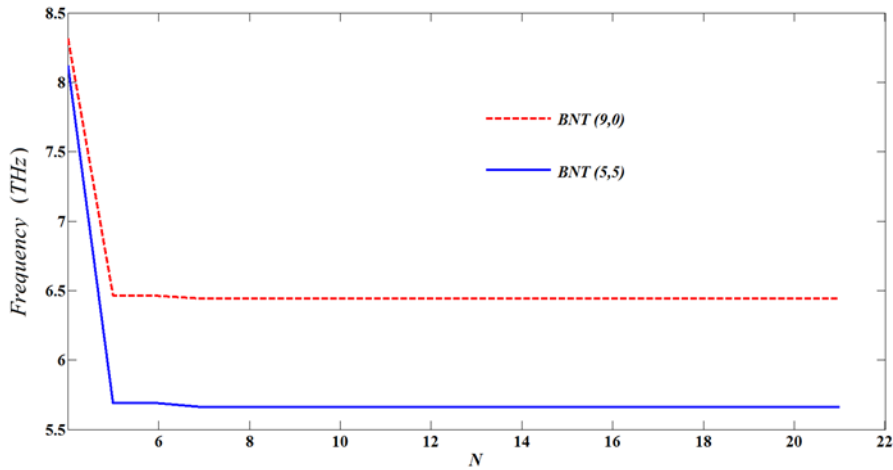


Fig. 3 The number of nodes required for the convergence of the problem

Table 2 Comparison of molecular dynamics simulation results with reference (Chandra *et al.* 2015)

	Frequency (THz)					
	Present study	Ref (Chandra <i>et al.</i> 2015)	Present study	Ref (Chandra <i>et al.</i> 2015)	Present study	Ref (Chandra <i>et al.</i> 2015)
	$T = 100 K$		$T = 400 K$		$T = 1000 K$	
1th Mode	0.52	0.52	0.51	0.50	0.49	0.49
2th Mode	1.08	1.08	1.06	1.07	1.02	1.02
3th Mode	1.71	1.73	1.68	1.69	1.63	1.63
4th Mode	2.31	2.33	2.27	2.27	2.20	2.17

Table 3 Comparison of frequency of BNNT with reference (Yang *et al.* 2010)

N	Frequency						
	5	6	7	8	10	16	20
Present study	0.81595	0.81223	0.80494	0.80548	0.80548	0.80548	0.80548
Ref (Yang <i>et al.</i> 2010)	0.81629	0.81256	0.80536	0.80550	0.80551	0.80551	0.80551

Table 4 Comparison of result in the different models

	Frequency of BNT (9,0) - (THz)		
	$E = 0 (V/A^\circ)$	$E = 0.185 (V/A^\circ)$	$E = 0.37 (V/A^\circ)$
MD	1.795	1.790	1.785
Classical continuum mechanic	15.395	11.936	6.602
Surface elasticity theory	1.797	1.790	1.785
$\lambda_s + 2\mu_s (N/m)$	-20.499	-16.7	-7.5
$\tau_s (N/m)$	-0.042	-0.026	-0.0157

Table 5 Comparison of result in the different models

	Frequency of BNT (9,0) - (THz)		
	$E = 0 (V/A^\circ)$	$E = 0.185 (V/A^\circ)$	$E = 0.37 (V/A^\circ)$
MD	1.625	1.625	1.625
Classical continuum mechanic	15.238	15.238	15.238
Surface elasticity theory	1.625	1.625	1.625
$\lambda_s + 2\mu_s (N/m)$	20	20	20
$\tau_s (N/m)$	-0.091	-0.091	-0.091

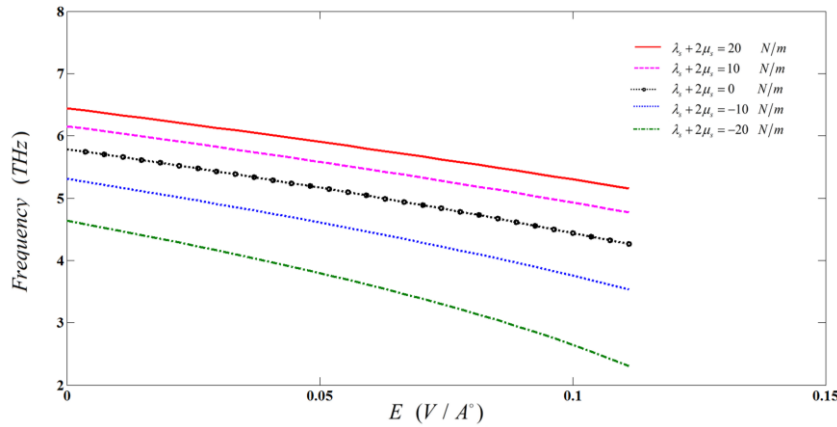


Fig. 4 Natural frequency of zigzag BNNTs in different electric fields

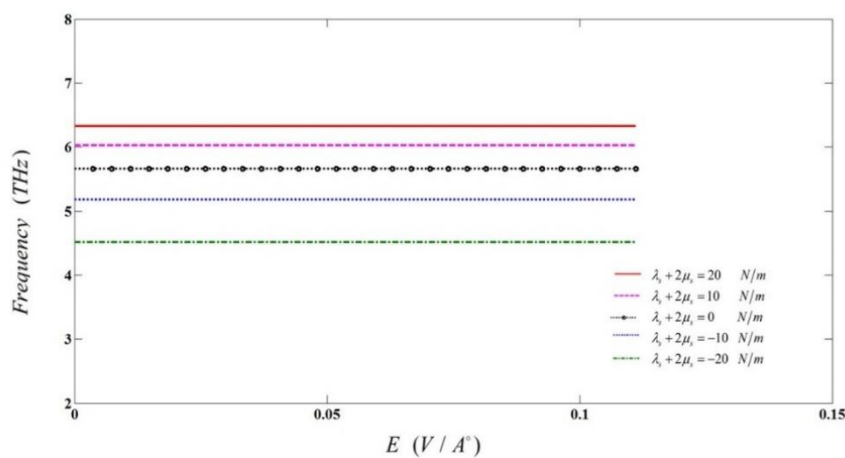


Fig. 5 Natural frequency of Armchair BNNTs in different electric fields

$n = 10$. In these results, the length of the BNNT is considered 4 nm.

In Table 2, the natural frequencies of BNNT (10, 10) at different temperatures are compared with reference (Chandra *et al.* 2015). In this reference, the natural frequency of BNNT with a length of 6.9 nm in three different temperatures is calculated by using the molecular dynamics method. The results of this paper are fitted with the above reference.

In Table 3, the vibrations of BNNTs (8, 0) in different numbers of nodes are investigated. The natural frequency is calculated without considering the surface effect. These results are compared with the reference (Yang *et al.* 2010). In this reference, the natural frequencies of the BNNTs are obtained by using the Timoshenko beam model and the DQM that the results of this paper are fitted with the reference.

In Tables 4 and 5, the results of molecular dynamics, classical continuum mechanics, and surface elasticity theory for the natural frequency of two types of BNNTs under an electric field are compared. As can be observed, due to the non-consideration of the effects of surface parameter, the results in classical continuum mechanics are different from the non-classical continuum mechanics. However, these results in the surface elasticity theory for different values of surface stress and surface elastic modulus are well fitted

with the molecular dynamics method, representing the effective performance of surface elasticity theory in precise calculations of the vibrational behavior of nanostructures. According to the tables, it can be inferred that the surface elasticity theory could be an alternative and suitable method for the molecular dynamics method with fewer computations and acceptable results in predicting the vibration behavior of nanostructures.

4.2 Effect of electric field on the vibration of BNNTs

In Figs. 4 and 5, the effect of the electric field on the natural frequency of the zigzag and armchair BNNTs in different surface elasticity modulus is investigated, respectively. The length of the BNNT is considered 4 nm. To calculate the natural frequency applying the continuum mechanics, the mechanical and physical properties in the reference (Verma *et al.* 2007) are used. By increasing the electric field, the natural frequency of the zigzag BNNT enhances. Indeed, by applying an electric field in the zigzag BNNTs, it generates an axial force. Considering the motion equations, the dependence of the electric field on the zigzag BNNTs has been demonstrated. According to the achieved results, increasing the electric field does not affect the natural frequency of the armchair BNNT. Applying an electric field to the armchair BNNTs generates a torque

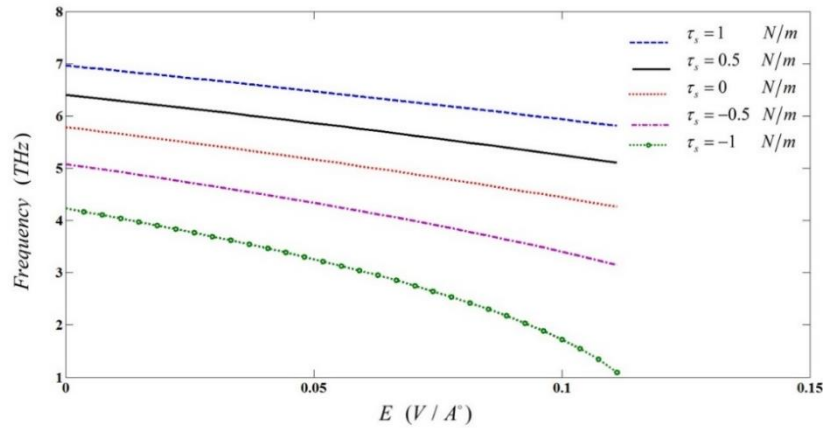


Fig. 6 Natural frequency of zigzag BNNTs in different surface stress

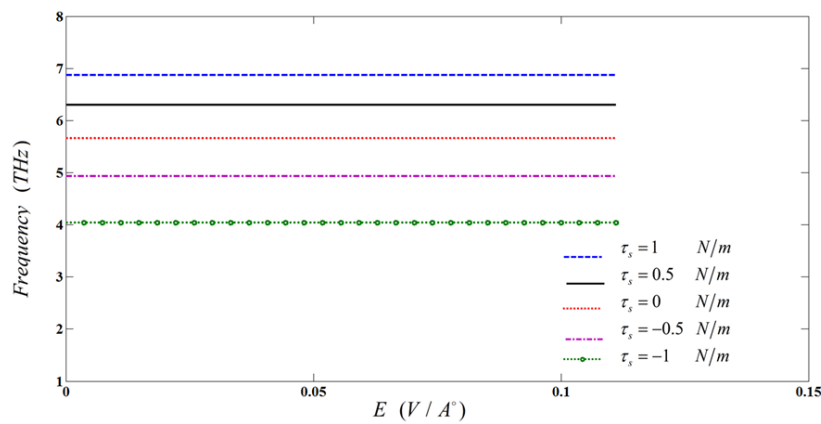


Fig. 7 Natural frequency of armchair BNNTs in different surface stress

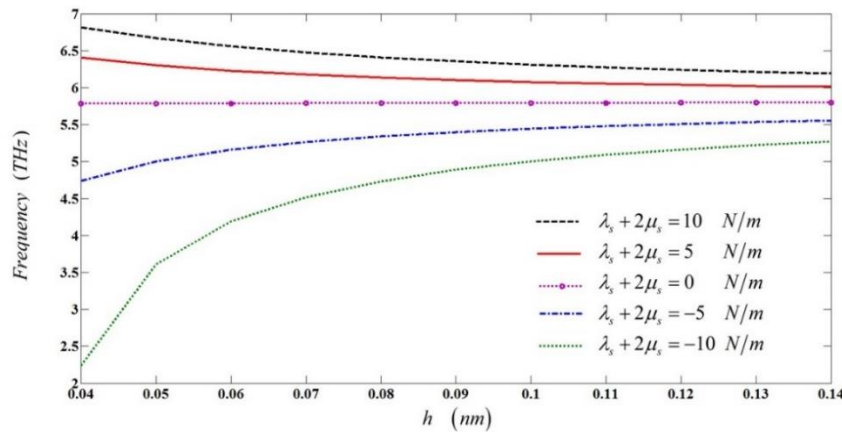


Fig. 8 Natural frequency of zigzag BNNTs in different surface elasticity modulus

force in it. The non-dependence of the electric field on natural frequency is obtained in Eq. (31). Furthermore, by increasing the surface elasticity modulus, the natural frequency of the BNNT has enhanced, which represents an increase in the rigidity of the BNNT in the higher modulus of elasticity.

As can be seen in the figures, the effect of the electrical field is dependent on the type of the chirality of the BNNTs. That is, regarding the chirality in zigzag BNNTs, the changes in the electric field affect the natural frequency. However, it has negligible effects on the armchair BNNTs.

4.3 Effect of surface stress on the vibration of BNNTs

In Figs. 6 and 7, the effect of surface stress on the natural frequency of zigzag and armchair BNNTs in different electric fields is investigated, respectively. In this case, the length of the BNNT is also considered 4 nm. According to the obtained results, the rigidity of the BNNT enhances by increasing the surface stress, and thus, the natural frequency in both BNNTs increases. Based on Fig. 6, the effect of declining the electric field is more tangible in lower stresses, which is because of reducing the rigidity of BNNTs in lower surface stresses.

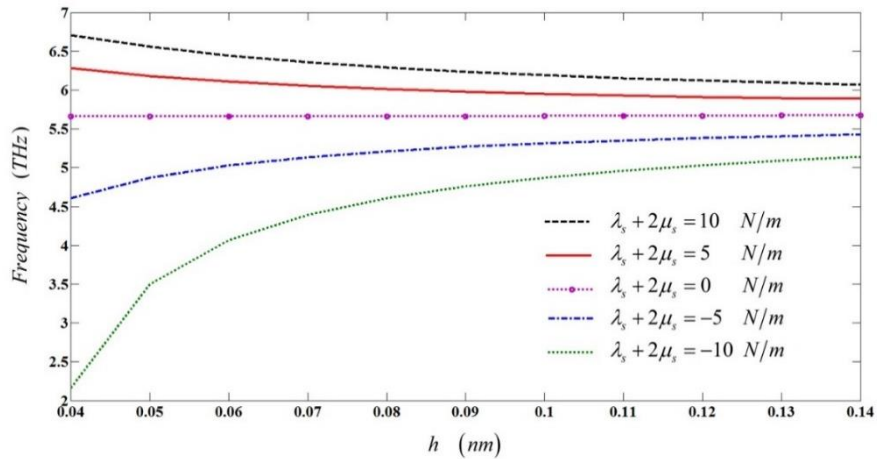


Fig. 9 Natural frequency of Armchair BNNTs in different surface elasticity modulus

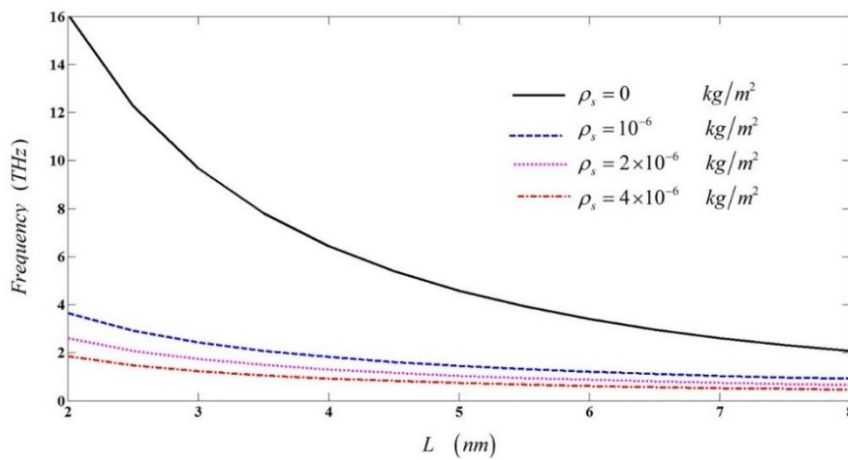


Fig. 10 Natural frequency of zigzag BNNTs in different length and surface density

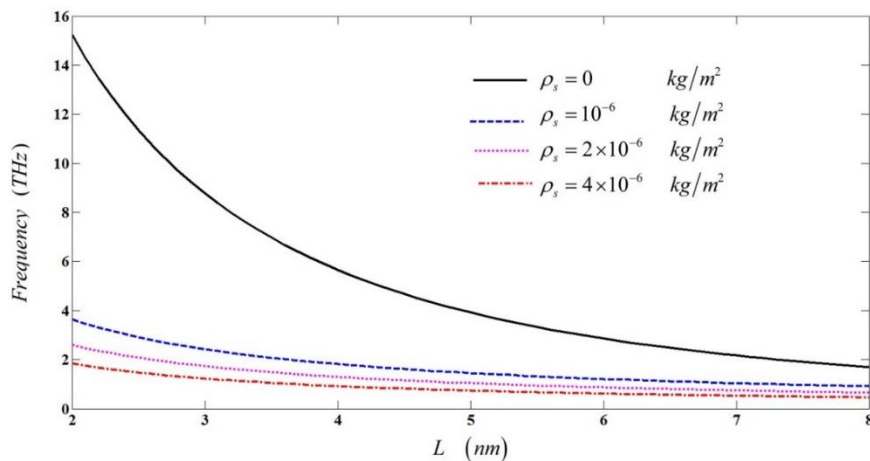


Fig. 11 Natural frequency of armchair BNNTs in different length and surface density

4.4 Effect of surface elasticity modulus on the vibration of BNNTs

In Figs. 8 and 9, the effect of surface elasticity modulus on the natural frequency of zigzag and armchair BNNTs in various thicknesses is investigated. In this case, the length of the BNNT is also considered 4 nm. According to the obtained results, increasing the surface

elasticity modulus at higher thicknesses of the BNNT has less impact on the natural frequency of the BNNT. By increasing the surface elasticity modulus, the natural frequency enhances, which is because of the increased rigidity of the BNNT. Indeed, the effect of the surface elasticity modulus on the natural frequency of the BNNT is higher in lower thicknesses, indicating the dependence of the BNNT on the surface effect in smaller dimensions. For

of surface elastic constants having positive values, an increase in the thickness causes a decrease in the frequency. In contrast, for elastic constants of surfaces with negative values, as the thickness increases, the natural frequency increases. According to the obtained results, the rigidity of the BNNT increases or decreases by the sign of surface elastic constants.

4.5 Effect of length and surface density on the vibration of BNNTs

In Figs. 10 and 11, the effect of BNNT length on natural frequency in different surface densities is investigated. Fig. 10 is related to the zigzag BNNT, and Fig. 11 is related to the armchair BNNT. According to the results achieved, the natural frequency declines with increasing the length of the BNNTs. The reason for decreasing natural frequency in higher lengths is the reduction in the rigidity of the BNNT. As well as the effect of the surface density on the natural frequency of the BNNT is higher in smaller lengths, which represents the dependence of smaller dimensions on the surface density. By comparing the two figures, it can be concluded that the natural frequency in the zigzag BNNT is higher than that in the armchair BNNT, which reflects the more rigidity of zigzag BNNT than the armchair BNNT.

5. Conclusions

In this paper, the effect of the electric field on the natural frequency of BNNTs is investigated by using the surface elasticity theory. The results are compared with the molecular dynamics simulation. The Timoshenko beam model is adopted to model BNNT. The equations of motion and boundary conditions are obtained by applying Hamilton's principle. Then, the DQM is exploited to discretize the equations of motion and solve the vibration problem through clamped-guided boundary conditions. The innovation of this paper is the study of the electric field effect and the size effect in surface elasticity theory on the vibrations of BNNTs, which has less attracted the attention of researchers. These results are calculated for the vibrations of two types of zigzag and armchair BNNTs. According to the results, the natural frequency enhances in the zigzag BNNT with increasing electric field, while the natural frequency does not change in the armchair BNNT. In fact, the electric field generates the axial force in the zigzag BNNT and the torque force in the armchair BNNT. Also, the effect of BNNT length and thickness on its vibrations is investigated.

The effect of the surface is more evident in the smaller dimensions. Indeed, the less the length and thickness of the BNNT, the effect of the surface on the BNNT will be more. As stated in the results, increasing surface elastic constant causes the natural frequency to increase due to the changes in the rigidity of the BNNT. The rigidity of the BNNT increases or decreases by the sign of surface elastic constants. Also, as the length of the nanotube increases, the rigidity of the nanotube decreases, resulting in a decrease in the frequency of the nanotube. The results of this paper are fitted with the molecular dynamics simulation, which

represents the effective performance of surface elasticity theory in accurate calculations of vibrational behavior of nanostructures. Finally, it should be noted that the results of the surface elasticity with high accuracy can be employed as an alternative method of molecular dynamics to model the vibrations of BNNTs.

References

- Ahmed, R.A., Al-Maliki, A.F. and Faleh, N.M. (2020), "Dynamic characteristics of multi-phase crystalline porous shells with using strain gradient elasticity", *Adv. Nano Res.*, **8**(2), 157-167. <https://doi.org/10.12989/anr.2020.8.2.157>.
- Ajori, S. and Ansari, R. (2014), "Torsional buckling behavior of boron-nitride nanotubes using molecular dynamics simulations", *Curr. Appl Phys.*, **14**(8), 1072-1077. <https://doi.org/10.1016/j.cap.2014.06.001>.
- Al-Furjan, M., Habibi, M., Chen, G., Safarpour, H., Safarpour, M. and Tounsi, A. (2020a), "Chaotic simulation of the multi-phase reinforced thermo-elastic disk using GDQM", *Eng. Comput.* 1-24. <https://doi.org/10.1007/s00366-020-01144-2>.
- Al-Furjan, M., Habibi, M., Ni, J., won Jung, D. and Tounsi, A. (2020b), "Frequency simulation of viscoelastic multi-phase reinforced fully symmetric systems", *Eng. Comput.* 1-17. <https://doi.org/10.1007/s00366-020-01200-x>.
- Al-Furjan, M., Habibi, M., Won Jung, D., Sadeghi, S., Safarpour, H., Tounsi, A. and Chen, G. (2020c), "A computational framework for propagated waves in a sandwich doubly curved nanocomposite panel", *Eng. Comput.* 1-18. <https://doi.org/10.1007/s00366-020-01130-8>.
- Al-Furjan, M., Safarpour, H., Habibi, M., Safarpour, M. and Tounsi, A. (2020d), "A comprehensive computational approach for nonlinear thermal instability of the electrically FG-GPLRC disk based on GDQ method", *Eng. Comput.* 1-18. <https://doi.org/10.1007/s00366-020-01088-7>.
- Al-Furjan, M.S.H., Habibi, M., Shan, L. and Tounsi, A. (2021a), "On the vibrations of the imperfect sandwich higher-order disk with a lactic core using generalize differential quadrature method", *Compos. Struct.*, **257**, 113150. <https://doi.org/10.1016/j.compstruct.2020.113150>.
- Al-Furjan, M., Habibi, M., Ghabussi, A., Safarpour, H., Safarpour, M. and Tounsi, A. (2021b), "Non-polynomial framework for stress and strain response of the FG-GPLRC disk using three-dimensional refined higher-order theory", *Eng. Struct.*, **228**, 111496. <https://doi.org/10.1016/j.engstruct.2020.111496>.
- Alimirzaei, S., Mohammadimehr, M. and Tounsi, A. (2019), "Nonlinear analysis of viscoelastic micro-composite beam with geometrical imperfection using FEM: MSGT electro-magneto-elastic bending, buckling and vibration solutions", *Struct. Eng. Mech.*, **71**(5), 485-502. <https://doi.org/10.12989/sem.2019.71.5.485>.
- Ansari, R., Mohammadi, V., Shojaei, M.F., Gholami, R. and Sahmani, S. (2014), "On the forced vibration analysis of Timoshenko nanobeams based on the surface stress elasticity theory", *Compos. Part B Eng.*, **60**, 158-166. <https://doi.org/10.1016/j.compositesb.2013.12.066>.
- Ansari, R., Gholami, R., Norouzzadeh, A. and Darabi, M. (2015), "Surface stress effect on the vibration and instability of nanoscale pipes conveying fluid based on a size-dependent Timoshenko beam model", *Acta Mech. Sin.*, **31**(5), 708-719. <https://doi.org/10.1007/s10409-015-0435-4>.
- Asghar, S., Naeem, M.N., Hussain, M., Taj, M. and Tounsi, A. (2020), "Prediction and assessment of nonlocal natural frequencies of DWCNTs: Vibration analysis", *Comput. Concr.*, **25**(2), 133-144. <https://doi.org/10.12989/cac.2020.25.2.133>.
- Atabakhshian, V. and Shoostaria, A. (2020), "A study on the

- dynamic instabilities of a smart embedded micro-shell induced by a pulsating flow: A nonlocal piezoelectric approach”, *Adv. Nano Res.*, **9**(3), 133-145.
<https://doi.org/10.12989/anr.2020.9.3.133>.
- Attia, M.A. (2017), “On the mechanics of functionally graded nanobeams with the account of surface elasticity”, *Int. J. Eng. Sci.*, **115**, 73-101. <https://doi.org/10.1016/j.ijengsci.2017.03.011>.
- Balubaid, M., Tounsi, A., Dakhel, B. and Mahmoud, S. (2019), “Free vibration investigation of FG nanoscale plate using nonlocal two variables integral refined plate theory”, *Comput. Concr.*, **24**(6), 579-586.
<https://doi.org/10.12989/cac.2019.24.6.579>.
- Bellal, M., Hebali, H., Heireche, H., Bousahla, A.A., Tounsi, A., Bourada, F., Mahmoud, S., Bedia, E. and Tounsi, A. (2020), “Buckling behavior of a single-layered graphene sheet resting on viscoelastic medium via nonlocal four-unknown integral model”, *Steel Compos. Struct.*, **34**(5), 643-655.
<https://doi.org/10.12989/scs.2020.34.5.643>.
- Beni, Y.T. (2016), “Size-dependent analysis of piezoelectric nanobeams including electro-mechanical coupling”, *Mech. Res. Commun.*, **75**, 67-80.
<https://doi.org/10.1016/j.mechrescom.2016.05.011>.
- Beni, Y.T., Zeverdejani, M.K. and Mehralian, F. (2017), “Buckling analysis of orthotropic protein microtubules under axial and radial compression based on couple stress theory”, *Math. Biosci.*, **292**, 18-29. <https://doi.org/10.1016/j.mbs.2017.07.002>.
- Berghouti, H., Adda Bedia, E., Benkhedda, A. and Tounsi, A. (2019), “Vibration analysis of nonlocal porous nanobeams made of functionally graded material”, *Adv. Nano Res.*, **7**(5), 351-364.
<https://doi.org/10.12989/anr.2019.7.5.351>.
- Blase, X., Rubio, A., Louie, S.G. and Cohen, M.L. (1994), “Stability and band gap constancy of boron nitride nanotubes”, *EPL*, **28**(5), 335-340.
<https://doi.org/10.1209/0295-5075/28/5/007>.
- Bourada, F., Bousahla, A.A., Tounsi, A., Bedia, E., Mahmoud, S., Benrahou, K.H. and Tounsi, A. (2020), “Stability and dynamic analyses of SW-CNT reinforced concrete beam resting on elastic-foundation”, *Comput. Concr.*, **25**(6), 485-495.
<https://doi.org/10.12989/cac.2020.25.6.485>.
- Bousahla, A.A., Bourada, F., Mahmoud, S., Tounsi, A., Algarni, A., Bedia, E. and Tounsi, A. (2020), “Buckling and dynamic behavior of the simply supported CNT-RC beams using an integral-first shear deformation theory”, *Comput. Concr.*, **25**(2), 155-166. <https://doi.org/10.12989/cac.2020.25.2.155>.
- Boutaleb, S., Benrahou, K.H., Bakora, A., Algarni, A., Bousahla, A.A., Tounsi, A., Tounsi, A. and Mahmoud, S. (2019), “Dynamic analysis of nanosize FG rectangular plates based on simple nonlocal quasi 3D HSDT”, *Adv. Nano Res.*, **7**(3), 191-208. <https://doi.org/10.12989/anr.2019.7.3.191>.
- Chandra, A., Patra, P.K. and Bhattacharya, B. (2015), “Thermal vibration characteristics of armchair boron-nitride nanotubes”, *J. Appl. Phys.*, **118**(23), 234503.
<https://doi.org/10.1063/1.4937559>.
- Chandra, A., Patra, P.K. and Bhattacharya, B. (2016), “Thermomechanical buckling of boron nitride nanotubes using molecular dynamics”, *Mater. Res. Express*, **3**(2), 025005.
<https://doi.org/10.1088/2053-1591/3/2/025005>.
- Civalek, O., Uzun, B. and Yayli, M.O. (2020), “Frequency, bending and buckling loads of nanobeams with different cross sections”, *Adv. Nano Res.*, **9**(2), 91-104.
<https://doi.org/10.12989/anr.2020.9.2.091>.
- De Rosa, M.A., Lippiello, M., Babilio, E. and Ceraldi, C. (2021), “Nonlocal vibration analysis of a nonuniform carbon nanotube with elastic constraints and an attached mass”, *Materials*, **14**(13), 3445. <https://doi.org/10.3390/ma14133445>.
- Dehshahri, K., Nejad, M.Z., Ziaee, S., Niknejad, A. and Hadi, A. (2020), “Free vibrations analysis of arbitrary three-dimensionally FGM nanoplates”, *Adv. Nano Res.*, **8**(2), 115-134. <https://doi.org/10.12989/anr.2020.8.2.115>.
- Draiche, K., Bousahla, A.A., Tounsi, A., Alwabri, A.S., Tounsi, A. and Mahmoud, S. (2019), “Static analysis of laminated reinforced composite plates using a simple first-order shear deformation theory”, *Comput. Concr.*, **24**(4), 369-378.
<https://doi.org/10.12989/cac.2019.24.4.369>.
- Ebrahimi, F. and Daman, M. (2016), “Investigating surface effects on thermomechanical behavior of embedded circular curved nanosize beams”, *J. Eng.*, 9848343.
<https://doi.org/10.1155/2016/9848343>.
- Ebrahimi, N. and Beni, Y.T. (2016), “Electro-mechanical vibration of nanoshells using consistent size-dependent piezoelectric theory”, *Steel Compos. Struct.*, **22**(6), 1301-1336.
<https://doi.org/10.12989/scs.2016.22.6.1301>.
- Esmaili, M. and Beni, Y.T. (2019), “Vibration and buckling analysis of functionally graded flexoelectric smart beam”, *J. Appl. Comput. Mech.*, **5**(5), 900-917.
<https://doi.org/10.22055/JACM.2019.27857.1439>.
- Faramoushjan, S.G., Jalalifar, H. and Kolahchi, R. (2021), “Mathematical modelling and numerical study for buckling study in concrete beams containing carbon nanotubes”, *Adv. Concr. Constr.*, **11**(6), 521-529.
<https://doi.org/10.12989/acc.2021.11.6.521>.
- Ghobadi, A., Beni, Y.T. and Żur, K.K. (2021a), “Porosity distribution effect on stress, electric field and nonlinear vibration of functionally graded nanostructures with direct and inverse flexoelectric phenomenon”, *Compos. Struct.*, **259**, 113220. <https://doi.org/10.1016/j.compstruct.2020.113220>.
- Ghobadi, A., Golestanian, H., Beni, Y.T. and Żur, K.K. (2021b), “On the size-dependent nonlinear thermo-electro-mechanical free vibration analysis of functionally graded flexoelectric nanoplate”, *Commun. Nonlinear Sci. Numer. Simul.*, **95**, 105585.
<https://doi.org/10.1016/j.cnsns.2020.105585>.
- Gurtin, M.E. and Murdoch, A.I. (1975), “A continuum theory of elastic material surfaces”, *Archive for Rational Mechanics and Analysis*, **57**(4), 291-323. <https://doi.org/10.1007/BF00261375>.
- Heidari, F., Taheri, K., Sheybani, M., Janghorban, M. and Tounsi, A. (2021), “On the mechanics of nanocomposites reinforced by wavy/defected/aggregated nanotubes”, *Steel Compos. Struct.*, **38**(5), 533-545. <https://doi.org/10.12989/scs.2021.38.5.533>.
- Heireche, H., Tounsi, A., Benzair, A., Maachou, M. and Adda Bedia, E.A. (2008), “Sound wave propagation in single-walled carbon nanotubes using nonlocal elasticity”, *Physica E*, **40**(8), 2791-2799. <http://doi.org/10.1016/j.physe.2007.12.021>.
- Hosseini-Hashemi, S. and Ilkhani, M.R. (2016), “Exact solution for free vibrations of spinning nanotube based on nonlocal first order shear deformation shell theory”, *Compos. Struct.*, **157**, 1-11. <https://doi.org/10.1016/j.compstruct.2016.08.019>.
- Huang, X., Hao, H., Oslub, K., Habibi, M. and Tounsi, A. (2021), “Dynamic stability/instability simulation of the rotary size-dependent functionally graded microsystem”, *Eng. Comput.* 1-17. <https://doi.org/10.1007/s00366-021-01399-3>.
- Hussain, M., Naeem, M.N., Tounsi, A. and Taj, M. (2019), “Nonlocal effect on the vibration of armchair and zigzag SWCNTs with bending rigidity”, *Adv. Nano Res.*, **7**(6), 431-442. <https://doi.org/10.12989/anr.2019.7.6.431>.
- Kang, J.H., Sauti, G., Park, C., Yamakov, V.I., Wise, K.E., Lowther, S.E., Fay, C.C., Thibault, S.A. and Bryant, R.G. (2015), “Multifunctional electroactive nanocomposites based on piezoelectric boron nitride nanotubes”, *Acs Nano*, **9**(12), 11942-11950. <https://doi.org/10.1021/acsnano.5b04526>.
- Karami, B., Janghorban, M. and Tounsi, A. (2019a), “Galerkin’s approach for buckling analysis of functionally graded anisotropic nanoplates/different boundary conditions”, *Eng. Comput.*, **35**(4), 1297-1316.
<https://doi.org/10.1007/s00366-018-0664-9>.

- Karami, B., Janghorban, M. and Tounsi, A. (2019b), "On pre-stressed functionally graded anisotropic nanoshell in magnetic field", *J. Braz. Soc. Mech. Sci. Eng.*, **41**(11), 1-17. <https://doi.org/10.1007/s40430-019-1996-0>.
- Karimipour, I., Beni, Y.T. and Zeighampour, H. (2020), "Vibration and dynamic behavior of electrostatic size-dependent micro-plates", *J. Braz. Soc. Mech. Sci. Eng.*, **42**(8), 1-22. <https://doi.org/10.1007/s40430-020-02490-4>.
- Karimipour, I., Beni, Y.T. and Akbarzadeh, A.H. (2019), "Size-dependent nonlinear forced vibration and dynamic stability of electrically actuated micro-plates", *Commun. Nonlinear Sci. Numer. Simul.*, **78**, 104856. <https://doi.org/10.1016/j.cnsns.2019.104856>.
- Karimipour, I., Beni, Y.T., Arvin, H. and Akbarzadeh, A. (2021), "Dynamic wave propagation in micro-torus structures: Implementing a 3D physically realistic theory", *Thin Wall Struct.*, **165**, 107995. <https://doi.org/10.1016/j.tws.2021.107995>.
- Khosravi, F., Simyari, M., Hosseini, S.A. and Tounsi, A. (2020), "Size dependent axial free and forced vibration of carbon nanotube via different rod models", *Adv. Nano Res.*, **9**(3), 157-172. <https://doi.org/10.12989/anr.2020.9.3.157>.
- Kim, J.H., Pham, T.V., Hwang, J.H., Kim, C.S. and Kim, M.J. (2018), "Boron nitride nanotubes: synthesis and applications", *Nano Converg.*, **5**(1), 1-13. <https://doi.org/10.1186/s40580-018-0149-y>.
- Lee, R.S., Gavillet, J., Chapelle, M.L.d.l., Loiseau, A., Cochon, J.L., Pigache, D., Thibault, J. and Willaime, F. (2001), "Catalyst-free synthesis of boron nitride single-wall nanotubes with a preferred zig-zag configuration", *Phys. Rev. B.*, **64**(12), 121405. <https://doi.org/10.1103/PhysRevB.64.121405>.
- López-Suárez, M., Abadal, G., Gammaitoni, L. and Rurali, R. (2015), "Noise energy harvesting in buckled BN nanoribbons from molecular dynamics", *Nano Energy*, **15** 329-334. <https://doi.org/10.1016/j.nanoen.2015.04.021>.
- Matouk, H., Bousahla, A.A., Heireche, H., Bourada, F., Bedia, E., Tounsi, A., Mahmoud, S., Tounsi, A. and Benrahou, K. (2020), "Investigation on hygro-thermal vibration of P-FG and symmetric S-FG nanobeam using integral Timoshenko beam theory", *Adv. Nano Res.*, **8**(4), 293-305. <https://doi.org/10.12989/anr.2020.8.4.293>.
- Meleshko, V. and Tokovyy, Y.V. (2013), "Equilibrium of an elastic finite cylinder under axisymmetric discontinuous normal loadings", *J. Eng. Math.*, **78**(1), 143-166. <https://doi.org/10.1007/s10665-011-9524-y>.
- Nakhmanson, S.M., Calzolari, A., Meunier, V., Bernholc, J. and Nardelli, M.B. (2003), "Spontaneous polarization and piezoelectricity in boron nitride nanotubes", *Phys. Rev. B.*, **67**(23), 235406. <https://doi.org/10.1103/PhysRevB.67.235406>.
- Ohba, N., Miwa, K., Nagasako, N. and Fukumoto, A. (2001), "First-principles study on structural, dielectric, and dynamical properties for three BN polytypes", *Phys. Rev. B.*, **63**(11), 115207. <https://doi.org/10.1103/PhysRevB.63.115207>.
- Ouakad, H.M., Sedighi, H.M. and Al-Qahtani, H.M. (2020), "Forward and backward whirling of a spinning nanotube nanorotor assuming gyroscopic effects", *Adv. Nano Res.*, **8**(3), 245-254. <https://doi.org/10.12989/anr.2020.8.3.245>.
- Pishkenari, H.N., Afsharmanesh, B. and Akbari, E. (2015), "Surface elasticity and size effect on the vibrational behavior of silicon nanoresonators", *Curr. Appl. Phys.*, **15**(11), 1389-1396. <https://doi.org/10.1016/j.cap.2015.08.002>.
- Rouabhia, A., Chikh, A., Bousahla, A.A., Bourada, F., Heireche, H., Tounsi, A., Kouider Halim, B., Tounsi, A. and Al-Zahrani, M.M. (2020), "Physical stability response of a SLGS resting on viscoelastic medium using nonlocal integral first-order theory", *Steel Compos. Struct.*, **37**(6), 695-709. <https://doi.org/10.12989/scs.2020.37.6.695>.
- Rubio, A., Corkill, J.L. and Cohen, M.L. (1994), "Theory of graphitic boron nitride nanotubes", *Phys. Rev. B.*, **49**(7), 5081. <https://doi.org/10.1103/PhysRevB.49.5081>.
- Sahmani, S., Aghdam, M. and Bahrami, M. (2016), "Surface free energy effects on the postbuckling behavior of cylindrical shear deformable nanoshells under combined axial and radial compressions", *Meccanica*, 1-24. <https://doi.org/10.1007/s11012-016-0465-4>.
- Sai, N. and Mele, E. (2003), "Microscopic theory for nanotube piezoelectricity", *Phys. Rev. B.*, **68**(24), 241405. <https://doi.org/10.1103/PhysRevB.68.241405>.
- Sedighi, H.M. and Bozorgmehri, A. (2016), "Dynamic instability analysis of doubly clamped cylindrical nanowires in the presence of Casimir attraction and surface effects using modified couple stress theory", *Acta Mech.*, **227**(6), 1575-1591. <https://doi.org/10.1007/s00707-016-1562-0>.
- Shariati, A., Ebrahimi, F., Karimiasl, M., Selvamani, R. and Toghroli, A. (2020a), "On bending characteristics of smart magneto-electro-piezoelectric nanobeams system", *Adv. Nano Res.*, **9**(3), 183-191. <https://doi.org/10.12989/anr.2020.9.3.183>.
- Shariati, A., Habibi, M., Tounsi, A., Safarpour, H. and Safa, M. (2020b), "Application of exact continuum size-dependent theory for stability and frequency analysis of a curved cantilevered microtubule by considering viscoelastic properties", *Eng. Comput.*, 1-20. <https://doi.org/10.1007/s00366-020-01024-9>.
- Shojaeian, M. and Beni, Y.T. (2015), "Size-dependent electromechanical buckling of functionally graded electrostatic nano-bridges", *Sensot. Actuat. A Phys.*, **232**, 49-62. <https://doi.org/10.1016/j.sna.2015.04.025>.
- Shu, C. (2000), *Differential Quadrature and Its Application in Engineering*, Springer.
- Streitz, F.H., Cammarata, R.C. and Sieradzki, K. (1994), "Surface-stress effects on elastic properties. I. Thin metal films", *Phys. Rev. B.*, **49**(15), 10699-10706. <https://doi.org/10.1103/PhysRevB.49.10699>.
- Tadi Beni, Y. (2016), "Size-dependent electromechanical bending, buckling, and free vibration analysis of functionally graded piezoelectric nanobeams", *J. Intell. Mater. Syst. Struct.*, **27**(16), 2199-2215. <https://doi.org/10.1177/1045389X15624798>.
- Thibeault, S.A., Fay, C.C., Sauti, G., Kang, J.H. and Park, C. (2020), *Radiation shielding materials containing hydrogen, boron and nitrogen*, Google Patents.
- Tiano, A.L., Park, C., Lee, J.W., Luong, H.H., Gibbons, L.J., Chu, S.H., Applin, S., Gnoffo, P., Lowther, S. and Kim, H.J. (2014), "Boron nitride nanotube: Synthesis and applications", *Proceeding of Nanosensors, Biosensors, and Info-Tech Sensors and Systems 2014*, **9060**, 906006, California, U.S.A. <https://doi.org/10.1117/12.2045396>.
- Timesli, A. (2020), "Buckling analysis of double walled carbon nanotubes embedded in Kerr elastic medium under axial compression using the nonlocal Donnell shell theory", *Adv. Nano Res.*, **9**(2), 69-82. <https://doi.org/10.12989/anr.2020.9.2.069>.
- Verma, V., Jindal, V. and Dharamvir, K. (2007), "Elastic moduli of a boron nitride nanotube", *Nanotechnology*, **18**(43), 435711. <https://doi.org/10.1088/0957-4484/18/43/435711>.
- Xu, X.J., Deng, Z.C., Zhang, K. and Meng, J.M. (2016), "Surface effects on the bending, buckling and free vibration analysis of magneto-electro-elastic beams", *Acta Mech.*, **227**(6), 1557-1573. <https://doi.org/10.1007/s00707-016-1568-7>.
- Yang, J., Ke, L.L. and Kitipornchai, S. (2010), "Nonlinear free vibration of single-walled carbon nanotubes using nonlocal Timoshenko beam theory", *Physica E*, **42**(5), 1727-1735. <https://doi.org/10.1016/j.physe.2010.01.035>.
- Zeighampour, H. and Beni, Y.T. (2014), "Cylindrical thin-shell model based on modified strain gradient theory", *Int. J. Eng. Sci.*, **78**, 27-47. <https://doi.org/10.1016/j.ijengsci.2014.01.004>.

- Zeighampour, H. and Tadi Beni, Y. (2014), "Size-dependent vibration of fluid-conveying double-walled carbon nanotubes using couple stress shell theory", *Physica E*, **61**, 28-39. <https://doi.org/10.1016/j.physe.2014.03.011>.
- Zeighampour, H. and Beni, Y.T. (2015), "Free vibration analysis of axially functionally graded nanobeam with radius varies along the length based on strain gradient theory", *Appl. Math. Model.* **39**(18), 5354-5369. <https://doi.org/10.1016/j.apm.2015.01.015>.
- Zeighampour, H., Beni, Y.T. and Mehralian, F. (2015), "A shear deformable conical shell formulation in the framework of couple stress theory", *Acta Mech.*, **226**(8), 2607-2629. <https://doi.org/10.1007/s00707-015-1318-2>.
- Zeighampour, H., Beni, Y.T. and Karimipour, I. (2017), "Wave propagation in double-walled carbon nanotube conveying fluid considering slip boundary condition and shell model based on nonlocal strain gradient theory", *Microfluid. Nanofluid.*, **21**(5), 85. <https://doi.org/10.1007/s10404-017-1918-3>.
- Zerrouki, R., Karas, A., Zidour, M., Bousahla, A.A., Tounsi, A., Bourada, F., Tounsi, A., Benrahou, K.H. and Mahmoud, S. (2021), "Effect of nonlinear FG-CNT distribution on mechanical properties of functionally graded nano-composite beam", *Struct. Eng. Mech.*, **78**(2), 117-124. <https://doi.org/10.12989/sem.2021.78.2.117>.
- Zevejdjani, M.K. and Beni, Y.T. (2020), "Effect of laminate configuration on the free vibration/buckling of FG Graphene/PMMA composites", *Adv. Nano Res.*, **8**(2), 103-114. <https://doi.org/10.12989/anr.2020.8.2.103>.
- Zhang, J. and Wang, C. (2014), "Effect of the electric field on the mechanical properties of gallium nitride nanowires", *EPL*, **105**(2), 28004. <https://doi.org/10.1209/0295-5075/105/28004>.
- Zhang, J., Wang, C. and Adhikari, S. (2013a), "Fracture and buckling of piezoelectric nanowires subject to an electric field", *J. Appl. Phys.*, **114**(17), 174306. <https://doi.org/10.1063/1.4829277>.
- Zhang, J., Wang, C. and Adhikari, S. (2013b), "Molecular structure-dependent deformations in boron nitride nanostructures subject to an electrical field", *J. Phys. D Appl. Phys.*, **46**(23), 235303. <https://doi.org/10.1088/0022-3727/46/23/235303>.
- Zhen, Y.X. (2017), "Wave propagation in fluid-conveying viscoelastic single-walled carbon nanotubes with surface and nonlocal effects", *Physica E*, **86**, 275-279. <https://doi.org/10.1016/j.physe.2016.10.037>.
- Zhi, C., Bando, Y., Tang, C., Honda, S., Kuwahara, H. and Golberg, D. (2006), "Boron nitride nanotubes/polystyrene composites", *J. Mater. Res.*, **21**(11), 2794-2800. <https://doi.org/10.1557/jmr.2006.0340>.
- Zhu, C.S., Fang, X.Q., Liu, J.X. and Li, H.Y. (2017), "Surface energy effect on nonlinear free vibration behavior of orthotropic piezoelectric cylindrical nano-shells", *Eur. J. Mech. A. Solid.*, **66**, 423-432. <https://doi.org/10.1016/j.euromechsol.2017.08.001>.
- Zong, Z. and Zhang, Y. (2009), *Advanced Differential Quadrature Methods*, CRC Press.